

## Activated Surface Diffusion in a Simple Colloid System

Minsu Kim,<sup>1</sup> Stephen M. Anthony,<sup>2</sup> and Steve Granick<sup>1,2,3</sup>

<sup>1</sup>*Departments of Physics, University of Illinois, Urbana, Illinois 61801, USA*

<sup>2</sup>*Departments of Chemistry, University of Illinois, Urbana, Illinois 61801, USA*

<sup>3</sup>*Departments of Materials Science and Engineering, University of Illinois, Urbana, Illinois 61801, USA*

(Received 15 August 2008; published 30 April 2009)

We investigate, from single-particle tracking of jumps, the cluster configurations that allow hopping over a geometric activation barrier in surface diffusion. Spherical colloidal particles, their dimers, and their isomeric planar trimers are compared on hexagonal surface lattices commensurate with the elemental size of one particle. The experiments reveal that translational and rotational mobility depend on the shape of these clusters, not only on their mass, because the jump process favors a restricted family of cluster configurations. The resulting strong decoupling between rotation and translation demonstrates the limitations of a naïve Arrhenius picture, even for a simple gravitational potential.

DOI: 10.1103/PhysRevLett.102.178303

PACS numbers: 82.70.Dd, 68.35.Fx

Activated hopping from site to site is a dominant mechanism of diffusion—its existence is taken for granted and it is enshrined in textbooks. Long central to the phenomenological interpretation of atomic motion in crystals and on crystal surfaces [1–5], potentially analogous behavior was discovered recently in biophysics regarding how lipid molecules diffuse on plasma membranes [6]. It is also central to theoretical understanding of energy dissipation in tribology [7,8]. A limitation on the experimental side is that the nature of what constitutes an elementary activated jump is problematic to measure directly. The role of size has been addressed most directly in the surface science of metal cluster mobility on surfaces [9–11], but atomic clusters change configuration and dissociate easily so that measurements of that kind inevitably reflect the motion of clusters in different configurations. In this study, we introduce a simple model system in which to quantify, one cluster at a time, how colloidal particles of definite size and shape diffuse on a commensurate surface lattice. While the energy barrier in this study is gravitational, which has the advantage of allowing single-particle imaging of individual jumps over barriers that are easy to vary systematically, the principles derived here can be translated to other systems by substituting the appropriate potential energy barrier. We observe that mobility depends on the cluster shape, not just on its mass, showing the failure of a naïve Arrhenius picture and a decoupling between translational and rotational motion for systems where transition state pathway favors particular configurations.

Our approach is to study the surface diffusion of colloidal clusters after they sediment in aqueous suspension to near the bottom a sample cell that is patterned with a surface lattice of hexagonally-spaced barriers whose height requires these colloids to hop between them. The surface lattices are fabricated by colloidal templating. A droplet of aqueous colloidal particles, 3  $\mu\text{m}$  diameter (2% solid), is spread on a microscope slide cleaned with piranha

solution. A close-packed monolayer forms when the water evaporates. Upon coating with a thin film of  $\text{SiO}_2$  using electron beam deposition, the  $\text{SiO}_2$  also deposits at the spots between neighboring spheres. The colloidal monolayer is easily detached by mild ultrasonication in water. Left behind is a hexagonal configuration of  $\text{SiO}_2$  posts, analogous to the arrangement of a fcc (111) crystal, and their height is the thickness of the  $\text{SiO}_2$  film, 50–300 nm, in

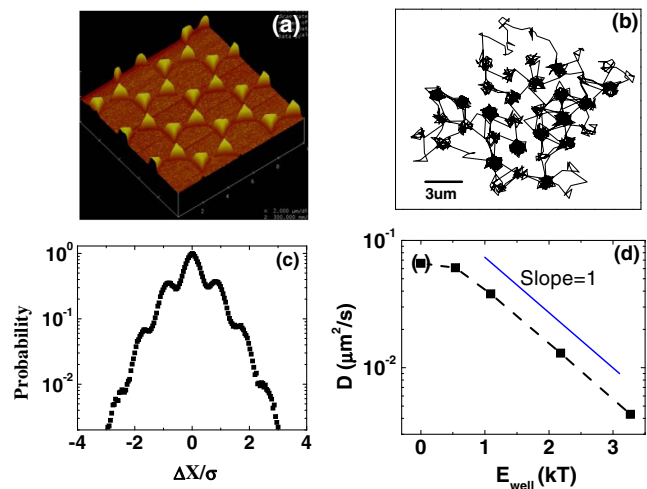


FIG. 1 (color online). (a) AFM image of a surface lattice prepared as described in text. (b) Representative trajectory of a spherical particle with diameter  $\sigma = 3 \mu\text{m}$  for 200 nm thick well height (4 h). The sample cell size is much larger than the range of motion depicted here; thus, these data are not influenced by boundaries. (c) Probability distribution of displacement ( $\Delta t = 200 \text{ sec}$ ) from the data in panel b. (d) Long-time diffusion coefficient of this particle as a function of the height of the lattice barriers ( $E_{\text{well}}$ ). The datum for smallest  $E_{\text{well}}$  is in parenthesis because for the reasons discussed in the text, there is no significant barrier to diffusion until  $E_{\text{well}} > 0.5 \text{ kT}$ .

the experiments presented below. A representative atomic force microscope (AFM) image is shown in Fig. 1(a).

To create clusters, the procedure is the same except that the SiO<sub>2</sub> film is only 30 nm thick; this is negligible relative to the colloid size but large enough to bond colloids together. The ultrasonication step results in clusters of various sizes and the motion of desired ones is tracked in a microscope using a 63× air objective and recorded by a CCD camera (Andor Ixon). While for these experiments, we have chosen to use colloids of size commensurate with the well diameters, by varying the colloid size relative to the well diameter, a variety of incommensurate surface patternings could be produced, expanding the utility as a model system. The water contains salt (3 mM NaCl) to reduce the Debye screening length to 5 nm, negligible compared to the particle diameter. The images are analyzed using tracking programs described by us elsewhere [12,13]. In the graphs presented below, each datum represents the analysis of 5–7 different particles or clusters.

To illustrate raw data, consider how spherical particles hop along these corrugated surfaces. The representative trajectory of a single particle in Fig. 1(b) shows the discrete area visited during 4 hr. Displacement probability in Fig. 1(c) shows the quantization of positions. The energy barrier over which a particle hops to pass from one surface lattice site to the next is the gravitational potential and can be quantified from the density mismatch ( $\Delta\rho = 1 \text{ g/cm}^3$ ) and the well height, resulting in an energy barrier  $E_{\text{well}}$  of 0.011 kT per nanometer of well height for a 3  $\mu\text{m}$  particle. Throughout,  $E_{\text{well}}$  is expressed in terms of the barrier for a single particle, regardless of the number of particles in the cluster. Figure 1(d) shows that translational diffusion ( $D_T$ ) decreases exponentially as the energy barrier increases, consistent with the classical Arrhenius relation,  $D = D_0 \exp(-\frac{E_{\text{well}}}{kT})$ , where  $E_{\text{well}}$  is activation energy.

Only at first is it surprising that the diffusivity is nearly the same for the cases  $E_{\text{well}} = 0$  and  $E_{\text{well}} = 0.5 \text{ kT}$ . The reason is partly geometrical and partly entropic. First, owing to the curvature of the colloids, the triangular barriers do not contact the colloids until sufficiently high, and when shorter than this present no obstacle. Second, sufficient energy barriers must be present to constrain the colloids to lattice positions; prior to this point, the entropic advantage of having many orientations prevents the particles from being well localized. This is why when analyzing the trend of the data, we consider only the regime where  $E_{\text{well}} > 0.5 \text{ kT}$ .

Now contrast this to dimers. In Fig. 2(a), one sees that whereas  $D_R$  (rotation parallel to the surface) decreases exponentially with increasing energy barrier,  $D_T$  decreases even more strongly, slope close to 1.3 on the semilog scale. Both observations differ from the naïve expectation, that because the mass is twice that of a single particle, the slope on the semilog scale should be 2. Especially noteworthy is that the slope for rotational diffusion is unity, meaning that

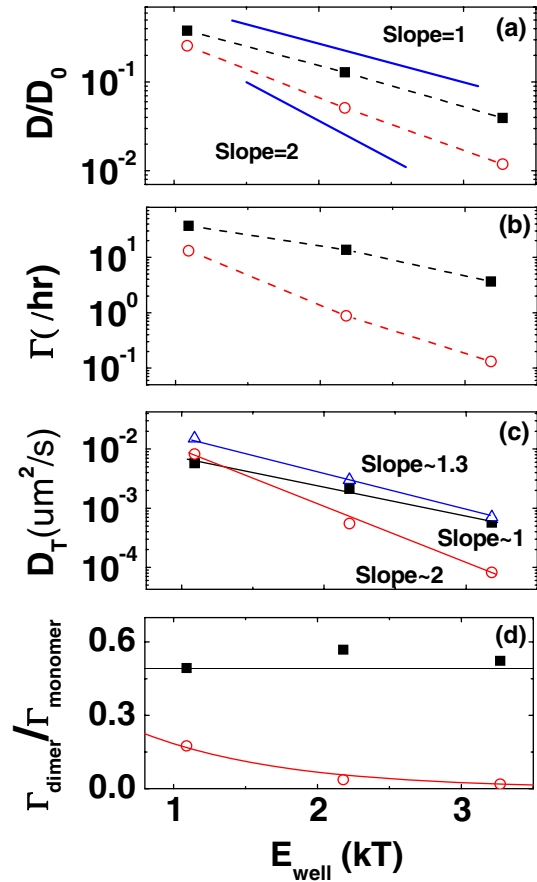


FIG. 2 (color online). Diffusion and jump frequency of a dimer of 3  $\mu\text{m}$  spheres, plotted in each panel against barrier height.  $D/D_0$  with no energy barrier are 0.66 and 0.71 for translation and rotation, respectively. Datum for surface corrugation of 0.53 kT is not included because hopping was not obstructed enough to distinguish different pathways. (a) Translational and rotational diffusion coefficients (open red circle and closed black square, respectively). (b) Jump frequency of zigzag and concerted motion (closed black squares and open red circles, respectively). (c) Overall translational diffusion (open blue triangles) separated into zigzag and concerted diffusion (closed black squares and open red circles, respectively). (d) Jump frequencies of a dimer normalized by those of a monomer.

a dimer's rotation has the same energy barrier as a monomer's translation.

Clearly, for dimers, translational and rotational diffusion are decoupled because positional jumps can take two pathways. They may be concerted: both ends hopping in unison over the same energy barrier. Or they may be zigzag: one end hopping, the other end swiveling behind. The frequencies ( $\Gamma$ ) of these respective alternatives were quantified from the raw data using the relation derived by Einstein and commonly used [1,14],  $D = \frac{a^2\Gamma}{4}$ , where  $a$  is jump distance. They are plotted against barrier height in Fig. 2(b).

As a pleasing check of consistency, we note that the sum of these two diffusion pathways adds to the measured macroscopic diffusion coefficients. Specifically, Fig. 2(c)

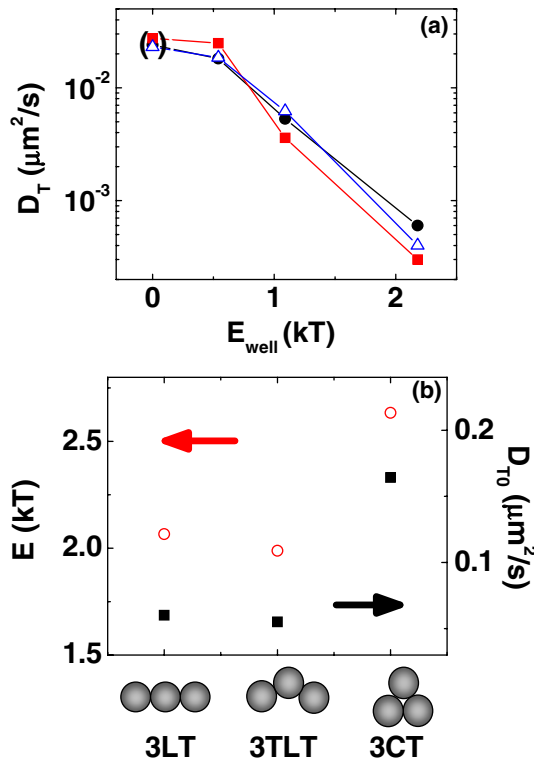


FIG. 3 (color online). Isomeric planar trimers composed of  $3 \mu\text{m}$  spheres. (a) Translational diffusion coefficients plotted semilogarithmically against barrier height ( $E_{\text{well}}$ ) for compact trimer (3CT), linear trimer (3LT), and tilted linear trimer (3TLT). These are closed red squares, closed black circles, and open blue triangles, respectively. Solid line is a guide to the eye. (b) The Arrhenius prefactors (closed black squares) and effective activation energy (open red circles) implied from data in panel (a).

shows that when the energy barrier was varied,  $D_T$  for zigzag motion dropped exponentially with slope  $-1$  as barrier height increased, just the same as for a single particle. This is because just one particle lifts up at a time and the second particle swivels behind. In contrast, the slope of  $D_T$  from the concerted jump pathway is 2 since this requires two particles up above the wells simultaneously. This explains why the macroscopic diffusion coefficient, which is the sum of these two, has the strange noninteger slope close to 1.3 in Fig. 2(c); it reflects the sum of two exponential decays. As for rotational motion, analysis of the raw data shows that only zigzag motion contributes to rotation of a dimer and this is why the measured rotational diffusion of a dimer has a slope of 1 in Fig. 2(a). The jump frequency of zigzag and concerted motion, plotted semilogarithmically against well height in Fig. 2(d), agrees with this notion.

Some of the experimental results for dimers can similarly be obtained theoretically from the Langevin equation; however, approximations must be made, the validity of which is not *a priori* evident without the experimental confirmation provided here. Namely, this approach is

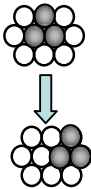
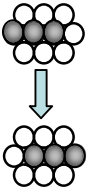
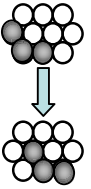
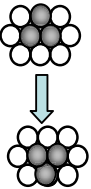
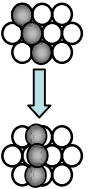
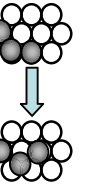
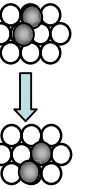
based on considering the known hydrodynamic interaction of a dimer with a flat plane, not the unknown interaction with the corrugated surface. However, given the excellent agreement between the experimental data and the theoretical approximation [black and red lines in Fig. 2(d)], the difference introduced by the corrugation does not appear to be significant. With regard to trimers, we are unaware of any analytical result even for a smooth plane.

Consider trimers experimentally now. Decoupling between translational and rotational diffusion was observed, just as described for dimers (not shown). Three planar isomers exist according to the angle between the two ends: linear trimer (LT,  $180^\circ$ ), tilted trimer (TLT,  $120^\circ$ ) and compact trimer (CT,  $60^\circ$ ). Their respective translational diffusion coefficients ( $D_T$ ), plotted on semilog scales as a function of barrier height in Fig. 3(a), reveal a complex pattern in which the relative dependence on barrier height is nonmonotonic. For instance, CT diffuses most slowly for the largest barrier but most rapidly for the smallest barrier. Figure 3(a) also includes control experiments in which the surface had no corrugation at all. Describing these data in the language of an Arrhenius activation process, we deduce the prefactor ( $D_{T0}$ ) and the *effective* activation energy ( $E$ ), shown in Fig. 3(b).

To find the highest prefactor for the most compact shape is understandable because this smallest radius of gyration sustains the least hydrodynamic drag, but to understand the different activation energies requires examining the different jumping mechanisms summarized in Table I. The translation of a trimer's center of mass does not require all three of its elemental units to move in a concerted jump (although it can do so); translation of only two elemental units in a zigzag motion is also possible, as is translation of 1.5 elemental units. In Table I, the motion of a dimer is included.

The concerted jump, three particles moving to adjacent sites while keeping the same orientation, has essentially the same jump frequency regardless of isomeric shape, but the frequencies of zigzag motion differ. The compact trimer swivels two elemental particles up above the barriers wells and these two particles rotate  $60^\circ$  into neighboring wells; comparison with the dimer shows almost the same zigzag jump frequency. In contrast, the linear and tilted linear trimers can pass through transition states in which all three elementary particles are incommensurate with the surface lattice because particles sit off the center of the surface lattice. These shapes rotate  $30^\circ$  to this metastable state while lifting one elementary unit at one end above a barrier and the elementary unit in the middle to half the barrier height. That is why LT and TLT have a lower activation energy than the compact-shaped trimer. The influence on translational diffusion coefficient is more prominent, the higher the barrier height; this explains why, for the highest barrier height, the LT and TLT diffuse more rapidly than the compact-shaped trimer.

TABLE I. Comparison of surface hopping mechanisms for a dimer and three isomeric planar trimer clusters: compact (CT), linear (LT), and tilted linear (TLT). The top row shows that a hopping event may involve overall translation of 3, 2, or 1.5 elemental particles within the cluster. The accompanying jump frequency, number of jumps per hour, is tabulated for well heights of 100 and 200 nm ( $E_{\text{well}} = 1.1$  and  $2.2k_B T$ , respectively). Numbers in parentheses are standard deviation from multiple experiments.

	CT 3	LT 3	TLT 3	CT 2	LT 1	TLT 1	Dimer
							
100 nm barrier height	3.4(0.8)	2.4(0.7)	3.3(0.8)	12(2)	29(5)	28(6)	13(1)
200 nm barrier height	0.27(0.19)	0.29(0.13)	0.31(0.16)	0.87(0.16)	4.9(2.3)	3.9(1.5)	0.88(0.21)
$N$ of ptcls in motion	3	3	3	2	1.5	1.5	2

The hopping of colloidal clusters on a surface lattice affords a simple model system in which to visualize how elementary jump mechanisms produce a macroscopic diffusion coefficient in the long-time limit. In the study presented here to introduce the concept, we find that the influence of the surface lattice to be both energetic and entropic. The entropic part comes because hexagonal arrangement of the barriers causes a restricted family of cluster configurations to be favored during the jump process, as visualized here.

This work was supported by the National Science Foundation, NSF-CBET-0853737. S. A. acknowledges the NSF for financial support.

[1] R. W. Balluffi, S. M. Allen, and W. C. Carter, *Kinetics of Materials* (Wiley, Hoboken, 2005).

- [2] G. A. Somorjai, *Surface Chemistry and Catalysis* (Wiley, New York, 1994).
- [3] H. Zhang *et al.*, *Acta Mater.* **55**, 4527 (2007).
- [4] W. P. Gou *et al.*, *Phys. Rev. B* **71**, 174307 (2005).
- [5] G. Antczak and G. Ehrlich, *Surf. Sci. Rep.* **62**, 39 (2007).
- [6] A. Kusumi *et al.*, *Annu. Rev. Biophys. Biomol. Struct.* **34**, 351 (2005).
- [7] E. Riedo *et al.*, *Phys. Rev. Lett.* **91**, 084502 (2003).
- [8] B. N. J. Persson, *Sliding Friction: Physical Principles and Applications* (Springer, New York, 2000).
- [9] G. L. Kellogg, *Phys. Rev. Lett.* **73**, 1833 (1994).
- [10] J. Y. Yang *et al.*, *J. Phys. Chem. C* **112**, 2074 (2008).
- [11] Q. W. Liu *et al.*, *Surf. Sci.* **554**, 25 (2004).
- [12] S. M. Anthony, L. F. Zhang, and S. Granick, *Langmuir* **22**, 5266 (2006).
- [13] S. M. Anthony, M. Kim, and S. Granick, *Langmuir* **24**, 6557 (2008).
- [14] D. Nykypanchuk, H. H. Strey, and D. A. Hoagland, *Science* **297**, 987 (2002).